Electronic Supplementary Information

Programmed stereoselective assembly of DNA-binding helical metallopeptides

Ilaria Gamba, Gustavo Rama, Elizabeth Ortega-Carrasco, Jean-Didier Maréchal, José Martínez-Costas, M. Eugenio Vázquez and Miguel Vázquez López**

I. Gamba, G. Rama, Prof. M. Vázquez López. Departamento de Química Inorgánica and Centro Singular de Investigación en Química Biolóxica e Materiais Moleculares (CiQUS). Universidade de Santiago de Compostela, 15782 Santiago de Compostela. Spain. E-mail: miguel.vazquez.lopez@usc.es

E. Ortega-Carrasco, Dr. J.-D. Maréchal. Departament de Química. Universitat Autònoma de Barcelona, 08193 Cerdanyola. Spain.

Prof. J. Martínez-Costas. Departamento de Bioquímica y Biología Molecular, and Centro Singular de Investigación en Química Biolóxica e Materiais Moleculares (CiQUS). Universidade de Santiago de Compostela, 15782 Santiago de Compostela. Spain.

Prof. M. E. Vázquez. Departamento de Química Orgánica and Centro Singular de Investigación en Química Biolóxica e Materiais Moleculares (CiQUS). Universidade de Santiago de Compostela, 15782 Santiago de Compostela. Spain. E-mail: eugenio.vazquez@usc.es

1. General

All reagents were acquired from commercial sources: Dimethylformamide (DMF) and Trifluoroacetic acid (TFA) were purchased from *Scharlau*, CH_2Cl_2 from *Panreac*, CH_3CN from *Merck*, HBTU (O-Benzotriazole-*N,N,N′,N′*-tetramethyl-uronium-hexafluorophosphate) and HATU (2-(*1H*-7-azabenzotriazol-1-*yl*)-1,1,3,3-tetramethyluronium hexafluorophosphate methanaminium) from *GL Biochem* (Shanghai) Ltd. All other chemicals were purchased from *Sigma-Aldrich* or *Fluka*. All solvents were dry and synthesis grade, unless specifically noted. $(NH_4)Fe_2(SO_4)_2.6H_2O$ salt from *Sigma-Aldrich* was used as Fe(II) ion source.

Reactions were followed by analytical RP-HPLC with an Agilent 1100 series LC/MS using a *Luna C18* (250 x 4.60 mm) analytical column from *Phenomenex*. Standard conditions for analytical RP-HPLC consisted on a linear gradient from 15% to 95% of solvent B for 30 min at a flow rate of 1 mL/min (A: water with 0.1% TFA, B: acetonitrile with 0.1% TFA). Compounds were detected by UV absorption at 222, 254 and 310 nm. High-Performance Liquid Chromatography (HPLC) was performed using an *Agilent 1100* series Liquid Chromatograph Mass Spectrometer system. Analytical HPLC was run using a *Luna C18* (250 x 4.60 mm) reverse phase analytical column; compounds were detected by UV absorption at 222, 254 and 310 nm. The purification of the peptides was performed on a *Luna C18* (250 x 10 mm) semi-preparative reverse phase column from Phenomenex. The standard gradient used for analytical and semi-preparative HPLC was 90:10 to 50:50 over 30 min (water/acetonitrile, 0.1% TFA). Electrospray Ionization Mass Spectrometry (ESI/MS) was performed with an *Agilent 1100* Series LC/MSD VL model in positive scan mode using direct injection of the purified peptide solution into the MS. Peptides purification was performed by semi-preparative RP-HPLC with an Agilent 1100 series Liquid Chromatograph using a Luna 5u $C_{18}(2)$ 100A (5 μm, 10 × 250 mm) reverse-phase column from Phenomenex. Standard conditions for analytical and semi-preparative RP-HPLC consisted on an isocratic regime during the first 5 min, followed by a linear gradient from 10% to 50% of solvent B for 30 min (A: water 0.1% TFA, B: acetonitrile 0.1% TFA). Compounds were detected by UV absorption (222 nm) and by ESI^+−MS. The fractions containing the products were freeze-dried, and their identity was confirmed by ESI^+−MS and MALDI-TOF.

Electrospray Ionization Mass Spectrometry (ESI/MS) was performed with an Agilent 1100 Series LC/MS model in positive scan mode using direct injection of the purified peptide solution into the MS.

Matrix-assisted laser desorption/ionization mass spectrometry (MALDI/MS) was performed with a Bruker Autoflex MALDI/TOF model in positive scan mode by direct irradiation of the matrix-absorbed peptide.

UV measurements were made in a *Jasco V-630* spectrophotometer coupled to a *Jasco ETC-717* temperature controller, using a standard *Hellma* semi-micro cuvette (140.002-QS). Measurements were made at 20 ºC.

Luminescence experiments were made with a *Jobin-Yvon Fluoromax-3* fluorescence spectrometers (DataMax 2.20), coupled to a *Wavelength Electronics* LFI−3751 temperature controller. All measurements were made with a *Hellma* semi-micro cuvette (114F-QS) at 20 ºC.

Circular dichroism measurements were made with a *Jasco J-715* coupled to a *Neslab RTE-111* termostated water bath, using a *Hellma* 100-QS cuvette (2 mm light pass). Measurements were made at 20 ºC. Samples contained (300 μL) 10 mM PBS buffer (pH = 7.2), 50 μM of peptides; the successive additions of Fe(II) aliquots ($(NH_4)_2Fe(SO_4)_2 \cdot 6H_2O$, ammonium iron(II) sulfate (Mohr's salt), 3 μL, 10 mM aqueous solution) complete the complex formation (Fe(II), 100 μM). The spectra are the average of 2 scans and were processed using the program *Sigmaplot 11.0* (*Systat Software Inc*).

2. Synthesis of the unnatural coordinating residue Fmoc-O1PenBpy-OH (1)

The bipyridine residue was obtained following the route previously reported by us,[1] and which is based on a method reported by Newkome *et al.*[2], starting from 5,5'-diethyl-2,2'-bipyridine, which was obtained from 5,5-dimethil-2,2-bipyridine using the method reported by Francis H. Case[3] and Whittle *et al.*[4]

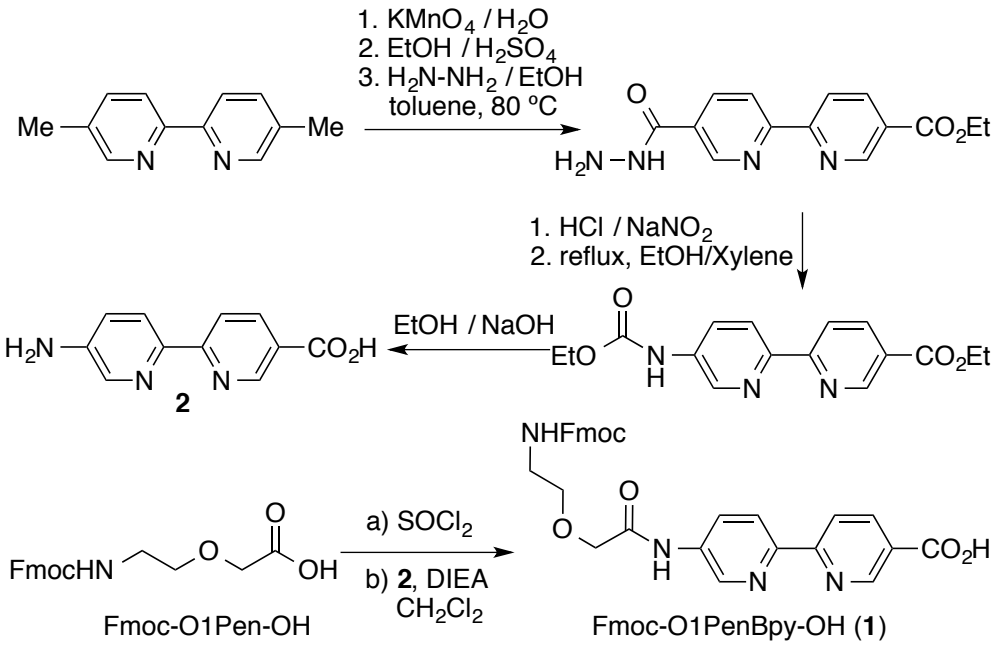

Scheme S1. *Synthesis of the coordinating amino acid **1**.*

3. Peptide synthesis

All peptide synthesis reagents and Fmoc amino acid derivatives were purchased from *GL Biochem* (Shanghai) Ltd. *Novabiochem*. Fmoc-O1Pen-OH was purchased from *IRIS Biotech* (Cat. #: FAA1565).

C-terminal amide peptides were synthesized following standard peptide synthesis protocols (Fmoc/tBu strategy) on a 0.05 mmol scale using a 0.48 mmol/g loading Fmoc-PAL-PEG-PS resin from *Life technologies* with a PS-3 automatic peptide synthesizer from *Protein Tecnologies*. The amino acids were coupled in 5-fold excess using HBTU as activating agent, except for the synthetic Fmoc-O1PenBpy-OH coordinating residue, which was coupled using HATU as activating agent.

Each amino acid was activated for 30 seconds in DMF before being added onto the resin and couplings were conducted for 30 min. Deprotection of the temporal Fmoc protecting group was performed by treating the resin with 20% piperidine in DMF for 10 min.

General procedure for cleavage-deprotection: A resin-bound peptide dried overnight (0.025 mmol) was placed in a 50 mL falcon tube, to which 3 mL of the cleavage cocktail (50 µL CH_2Cl_2, 25 µL of H_2O, 25 µL of TIS (Triisopropylsilane) and 940 TFA µL) were added. The resulting suspension was shaken for 3 h. The resin was filtered, and the TFA filtrate was concentrated with a nitrogen current to an approximate volume of 1 mL, which was added to ice-cold diethyl ether (10 mL). After 10 min, the precipitate was centrifuged and washed again with 15 mL of ice-cold ether. The solid residue was dried under argon and redissolved in acetonitrile/water 1:1 (1 mL) and purified by semi-preparative reverse-phase HPLC. The collected fractions were lyophilized and stored at −20 °C. Their identity was confirmed by ESI^+-MS and MALDI-TOF.

LL-H:

ESI-MS (*m/z*) $[M+H]^+$ calc for $C_{108}H_{113}N_{31}O_{24}$ = 2227.8; found = 1114.6, calc. for $[M+2H]^{2+}$ = 1114.9; found = 743.2, calc. for $[M+3H]^{3+}$ = 746.6.

UV (H_20) λ_{max}, nm (ε): 308 (169700) $M^{-1}cm^{-1}$

Yield: 52%

DD-H:

ESI-MS (*m/z*) $[M+H]^+$ calc for $C_{108}H_{113}N_{31}O_{24}$ = 2227.8; found = 1114.6, calc. for $[M+2H]^{2+}$ = 1114.9; found = 743.2, calc. for $[M+3H]^{3+}$ = 746.6.

UV (H_20) λ_{max}, nm (ε): 308 (169700) $M^{-1}cm^{-1}$

Yield: 43%

Synthesis of the fluorescent peptides

The coupling of the peptide with the rhodamine fluorescent probe was performed directly on the solid support: 5-(and-6)-carboxy-X-rhodamine (6.7 mg, 9.6 µmol), activated as succinimidyl ester, was dissolved

in 1.5 mL of DIEA solution in DMF (0.19 M, 0.29 mmol). The mixture was sonicated during 2 minutes and then loaded in a SPPS reactor, containing the Rink Amide resin (40 mg, 9.5 μmol) where the **LL-H** or **DD-H** peptides were previously grown, as described before. The mixture was gently shaken during 2 hours at rt. The resin was extensively washed and dried. The desired peptide was cleaved from the solid support, using the standard acidic cocktail (5 mL, 2.5 hrs), and purified by HPLC.

LL-RhH:

ESI-MS (*m/z*) $[M+H]^+$ calc for $C_{141}H_{142}N_{33}O_{28}$ = 2745,07; found = 1374.1, calc. for $[M+2H]^{2+}$ = 1373,5; found = 915.8, calc. for $[M+3H]^{3+}$ = 916.0. UV (H_20) λ_{max}, nm (ε): 575 (81000) $M^{-1}cm^{-1}$.

Yield: 54%

DD-RhH:

ESI-MS (*m/z*) $[M+H]^+$ calc for $C_{141}H_{142}N_{33}O_{28}$ = 2745,07; found = 1374.1, calc. for $[M+2H]^{2+}$ = 1373,5; found = 915.8, calc. for $[M+3H]^{3+}$ = 916.0. UV (H_20) λ_{max}, nm (ε): 575 (81,000) $M^{-1}cm^{-1}$.

Yield: 48%

The above described protocol was also followed to synthetize the corresponding fluorescein derivatives, using fluorescein isothiocyanate (FITC) as fluorescein source (Scheme S1).

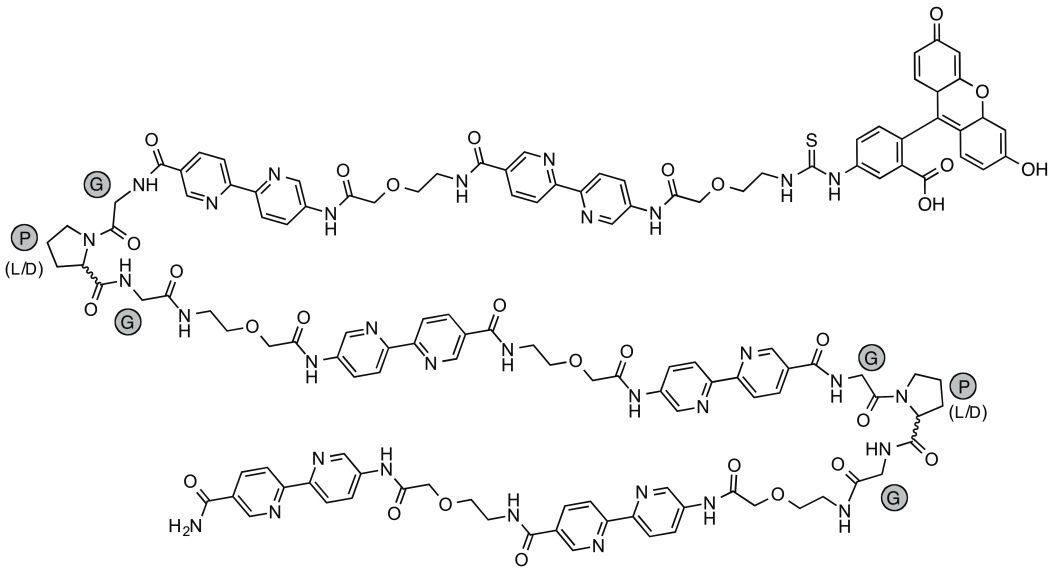

Scheme S2. *Structure of the peptide ligands functionalized with a fluorescein in the N-terminal end of their peptidic sequences (LL-FluH and DD-FluH).*

LL-FluH:

ESI-MS (*m/z*) $[M+H]^+$ calc for $C_{129}H_{126}N_{32}O_{29}S$ = 2618,91; found = 1310.5, calc. for $[M+2H]^{2+}$ = 1310,0; found = 873,6, calc. for $[M+3H]^{3+}$ = 873.9.

Yield: 57%

DD-FluH:

ESI-MS (*m/z*) $[M+H]^+$ calc for $C_{129}H_{126}N_{32}O_{29}S$ = 2618,91; found = 1310.5, calc. for $[M+2H]^{2+}$ = 1310,0; found = 873,6, calc. for $[M+3H]^{3+}$ = 873.9.

Yield: 53%

4. Peptide helicates synthesis

The peptide helicates were synthetized by addition of aliquots of an aqueous solution containing Fe(II) metal ions [Mohr's salt; the total amount of Fe(II) added was 2 equivalents] to a mother solution of the peptide ligand in PBS buffer (pH = 7.4, 298 K). All the coordination reactions were quantitative. The peptide helicates derived from the ligands **LL-FluH** and **DD-FluH** were poorly soluble in water.

5. MALDI-TOF mass spectrometry of the peptide helicates

ΔΔ-[Fe_2(**DD-H**)]$^{4+}$: MALDI-TOF (*m/z*) [M]$^+$ calc for $C_{108}Fe_2H_{113}N_{31}O_{24}$ = 2339.7, found = 2337.9

ΛΛ-[Fe_2(**LL-H**)]$^{4+}$: MALDI-TOF (*m/z*) [M]$^+$ calc for $C_{108}Fe_2H_{113}N_{31}O_{24}$ = 2339.7, found = 2337.9

ΔΔ-[Fe_2(**DD-RhH**)]$^{4+}$: MALDI-TOF (*m/z*) [M]$^+$ calc for $C_{141}H_{142}Fe_2N_{33}O_{28}$ = 2856,94, found = 2851.9

ΛΛ-[Fe_2(**LL-RhH**)]$^{4+}$: MALDI-TOF (*m/z*) [M]$^+$ calc for $C_{141}H_{142}Fe_2N_{33}O_{28}$ = 2856,94, found = 2854.8

ΔΔ-[Fe_2(**DD-FluH**)]$^{4+}$: MALDI-TOF (*m/z*) [M]$^+$ calc for $C_{129}H_{123}Fe_2N_{32}O_{29}S$ = 2727,78, found = 2727,5

ΛΛ-[Fe_2(**LL-FluH**)]$^{4+}$: MALDI-TOF (*m/z*) [M]$^+$ calc for $C_{129}H_{123}Fe_2N_{32}O_{29}S$ = 2727,78, found = 2727,5

6. Computational Details

Molecular Dynamics The optimization of the loop was performed on an initial model of the ΛΛ isomer where the metal centers satisfies the chiral induction. The simulation were performed under the UCSF chimera environment[5] using the MMTK Molecular Dynamics driver.[6] We used the built-in interface of UCSF Chimera for AmberTools,[7] to generate the GAFF force field of the system.[8] Its charges were generated through the Gasteiger method.[9] Considering that the first coordination sphere of the metal would not impact drastically on the dynamical properties of the loop, the simulations were performed in absence of metal and with the bipyridine rings fixed. A MD run of 50000 steps with an integration time of 1fs and 10000 of heating steps. The entire simulation was post-processed using the NMRCLUST on the production part of the simulation.[10] The 4 most populated clustered were selected for further calculations.

QM/MM refinement Quantum Mechanics/Molecular Mechanics geometry optimizations were performed using the ONIOM procedure as implemented in Gaussian09,[11,12] and combining DFT(B3LYP),[13,14] and AMBER force field.[7] For the total 279 atoms, the Quantum Mechanical part which includes the six bipyridine groups and the two Fe ions, is composed by 110 atoms. Two basis sets were used: 6-311G* [15,16] for the main group atoms and aug-cc-pVTZ for the Fe centres.[17] All calculations have been carried out using implicit solvent (water in this case) with the CPCM model,[18,19] and electronic embedding with the Fe atoms at the oxidation state +II and low spin.[20]

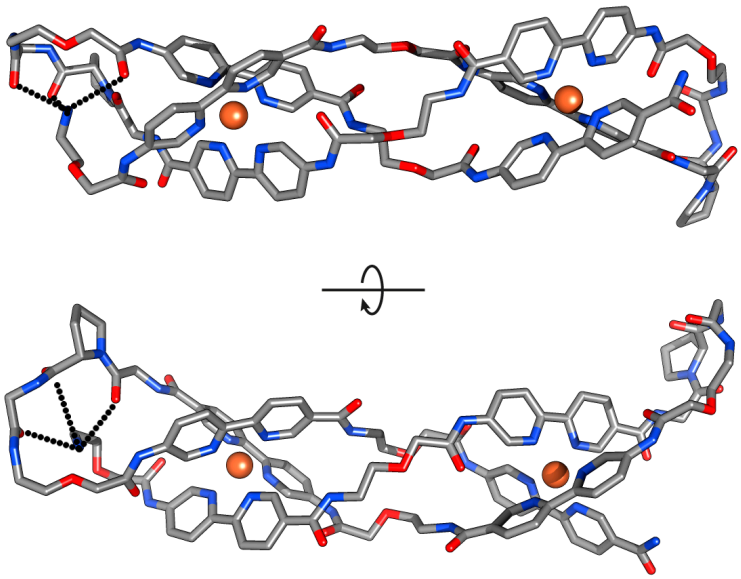

Figure S1. *Molecular representation of the most stable ΛΛ–[Fe$_2$(**LL-H**)]$^{4+}$ complex highlighting the interaction of the ammonium group of the N-terminal end with the C-terminal loop*

A total of 4 geometries were obtained that mainly differ from geometries of the loops and the *cis*/*trans* conformation of the amide groups in the loops and the spacers. The potential energy difference between the four geometries does not exceed 20 kJ/mol, which is consistent with a certain amount of flexibility of the system. For clarity, only the more stable complex was further analyzed.

The lowest energy model presents a helicoidal geometry (Figure S1) with both metal ions in octahedral configurations and the six bipyridine rings perfectly ordered around the metal centres.

The average distance between the Fe(II) ions and their coordinating nitrogen is 2.03 Å and the bipyridine groups present none to very little out-of-plane displacement (average value of 0.1 Å).

All the amino acid residues of the peptide ligand, including the two proline residues, present *trans* configuration. Despite their proximity, no hydrogen bonds are identified between the amide groups of the different spacers. The entire helicate is not perfectly symmetric, and both loops are oriented towards the same side of the helicate with an approximate angle of 75º with respect to the helicate axis. The two proline residues are at the most external part of the loops with atoms reaching up to 9 Å out of the helicate axis. Interestingly, the C-terminal proline (P_1, Scheme 1 in the main body of the manuscript) is less displaced from the helicate axis, and the entire C-terminal loop presents a more compact geometry as a result of the interaction of three carbonyl groups of the peptide backbone (G_1, P_1, G_2, Scheme 1) with the N-terminal amine, which is expected to be protonated at neutral pH (Figure S1). Altogether, it appears that a certain amount of molecular complexity and organization have been reached in this metallopeptide, since remote regions of the peptide chain are interacting with one another and influencing the folding of the system

7. Spectrophotometric studies (UV-Vis)

A solution of **LL-H** (4.4 μM), or **DD-H** (4.2 μM) in PBS buffer (pH 7.4, 298 K) was incubated with increasing concentrations of $(NH_4)_2Fe(SO_4)_2 \cdot 6H_2O$ (Mohr's salt) and the resulting titration profile measuring the absorbance at 550 nm was analyzed with the SpecFit program considering all the possible coordination equilibria between the peptide ligand and the metal ions (*i.e.* formation of 1:1, 1:2 and 2:1 species).

Spectrophotometric titration of LL-H with Fe(II)

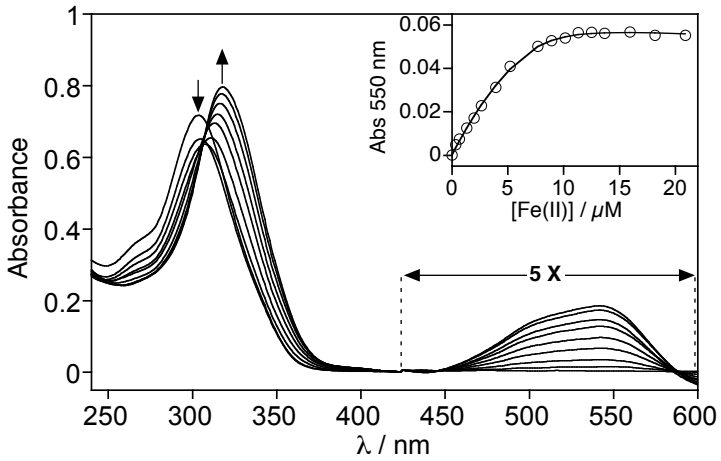

Figure S2. *UV/vis titration of a 4.4 μM solution of* ***LL-H*** *with increasing concentrations of Fe(II) in PBS buffer (pH = 7.4, 298 K). Inset shows the absorbance at 550 nm and the best fit to a mixed 1:1 and 2:1 binding model*

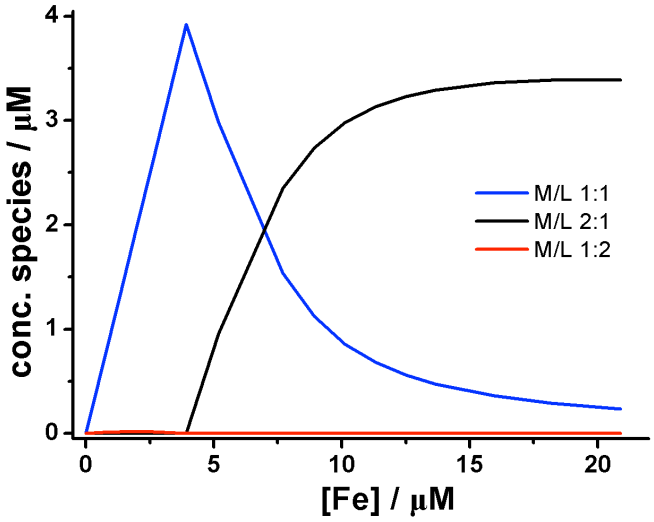

Figure S3. *Species distribution upon Fe(II) addition (**LL-H**). See figure S2 for the conditions of the titration.*

Spectrophotometric titration of DD-H with Fe(II)

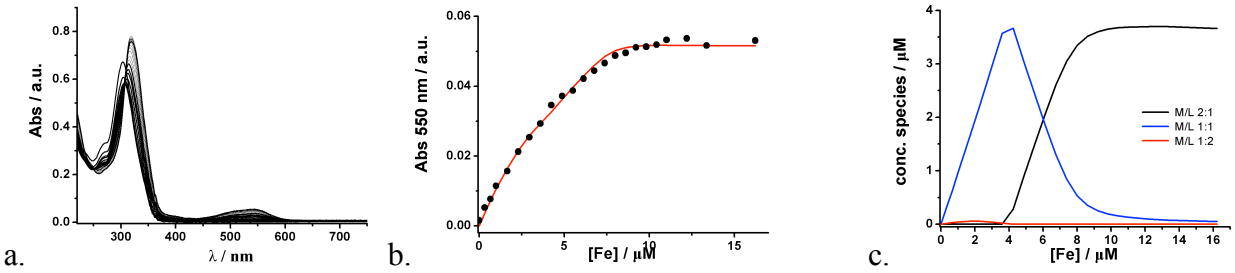

Figure S4. *a. Uv-vis spectra recorded upon titration of a 4.2 µM solution of DD-H with increasing concentrations of Fe(II) ions (PBS buffer, pH = 7.4, 298 K); b. plot Abs at 550 nm vs. [Fe]; c. species distribution upon Fe(II) addition.*

8. Circular dichroism

Circular dichroism measurements were made in a *Jasco J-715* CD spectrophotometer coupled to a *Neslab RTE-111* thermostated water bath, using a *Hellma* 100-QS cuvette (2 mm light pass). Measurements were made at 20ºC. Samples (300 μL, 10 mM PBS buffer, pH = 7.4) contained 50 μM of **LL-H** or **DD-H** peptides. The successive additions of Fe(II) aliquots [10 mM aqueous solution of $(NH_4)_2Fe(SO_4)_2 \cdot 6H_2O$ (Mohr's salt), aliquots of 3 μL] complete the formation of the complex (final [Fe(II)] = 100 μM). The spectra showed are the average of 2 scans and were processed using the program *Sigmaplot 11.0* (*Systat Software Inc*).

9. Fluorescence anisotropy titrations with three-way DNA junctions

A 1.0 mL solution of the peptidic helicate (ΔΔ-[Fe_2(**DD-RhH**)]$^{4+}$or ΛΛ-[Fe_2(**LL-RhH**)]$^{4+}$,1 μM) in 10 mM PBS buffer (10 mM NaCl, pH 7.3) was titrated with increasing concentrations of the $\mathbf{Y_1Y_2Y_3}$ DNA junction. The fluorescence anisotropy of the rhodamine fluorophore, measured at 611 nm, was recorded after each addition, and the resulting profile was analyzed using the program *DynaFit*, considering a 1:1 binding mode and the contribution of non-specific electrostatic complexes to the overall signal. The experiments were performed at 20 ºC in a 1 cm cuvette (excitation slit: 3 nm; emission slit: 10 nm; integration time 5 s).

10. Melting experiments

A deoxygenated solution the peptide helicate (ΔΔ-$[Fe_2(\mathbf{DD\text{-}H})]^{4+}$ or ΛΛ-$[Fe_2(\mathbf{LL\text{-}H})]^{4+}$, 7 μM) in 1 mL of 10 mM PBS buffer (10 mM NaCl, pH 7.2) was heated from 20 to 100 ºC, and the changes in absorbance at 525 nm (in the metal–ligand charge transfer region) were monitored. The transition between a well-folded structure and a disordered unfolded state was considered a two-state process, and therefore the corresponding unfolding equilibrium constant K, is equal to:

K = (fraction unfolded, f_u)/(fraction folded, f_f) = $f_u/(1- f_u)$; and: $f_u = (A_{obs}-A_f)/(A_u-A_f)$,

Where A_{obs} are the absorbance values, at 525 nm, recorded for each temperature during the transition, A_f is the absorbance of the folded helicate and A_u is the residual absorbance when the helicate is unfolded.

If we consider: ΔG = – R T ln K, and ΔG = ΔH – TΔS (R, gas constant), then we can extrapolate the thermodynamic parameters (ΔH, ΔS), associated to the folding event, from the slope (–ΔH/R) and the intercept (ΔS/R) of the linear plot: ln K *versus* 1/T (Van't Hoff plot). The melting temperatures reported were selected as the temperature at which half of the helicate is unfolded (K = 1; ΔG = 0).

Table S1. *Melting temperatures and thermodynamic parameters.*

	Tm, ºC	ΔH, kJmol^{-1}	ΔS, Jmol^{-1}
ΛΛ-$[Fe_2(\mathbf{LL\text{-}H})]^{4+}$	81.67	158.47	447.08
ΔΔ-$[Fe_2(\mathbf{DD\text{-}H})]^{4+}$	79.30	157.44	447.07

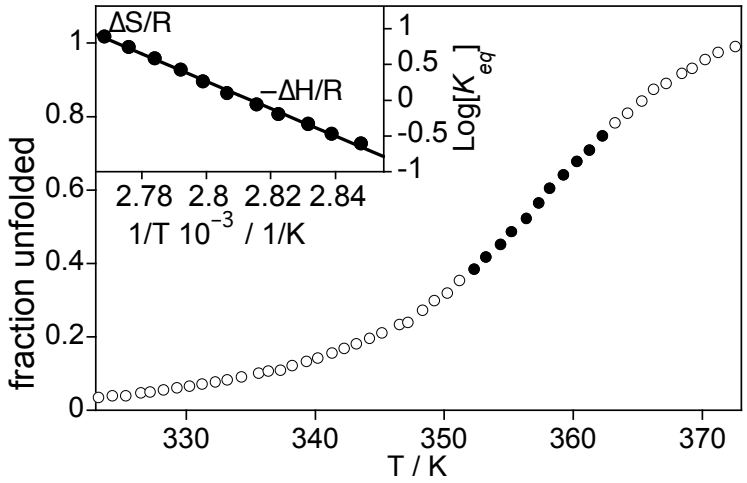

Figure S5. *Left: Thermal denaturation curve and Van't Hoff analysis of the thermal denaturation process of a 7 μM solution of ΛΛ–$[Fe_2(\mathbf{LL\text{-}H})]^{4+}$ in PBS buffer 10 mM, NaCl 10 mM, pH 7.2. Black points represent the data near the transition used in the Van't Hoff plot shown in the inset.*

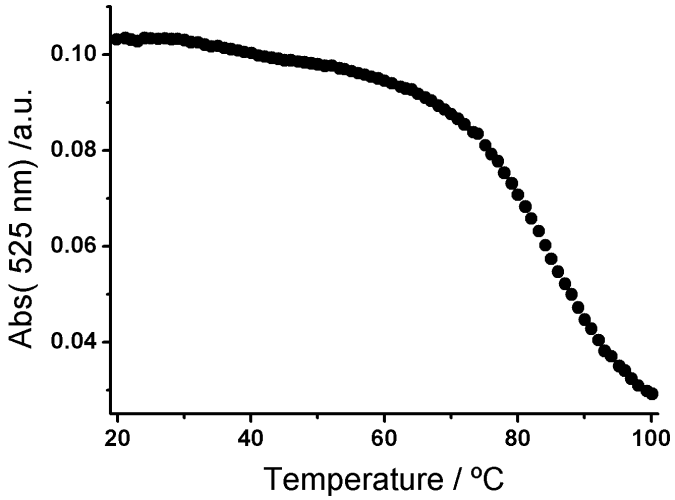

Figure S6. *ΛΛ-[Fe$_2$(**LL-H**)]$^{4+}$: Absorbance melting profile at 525 nm*

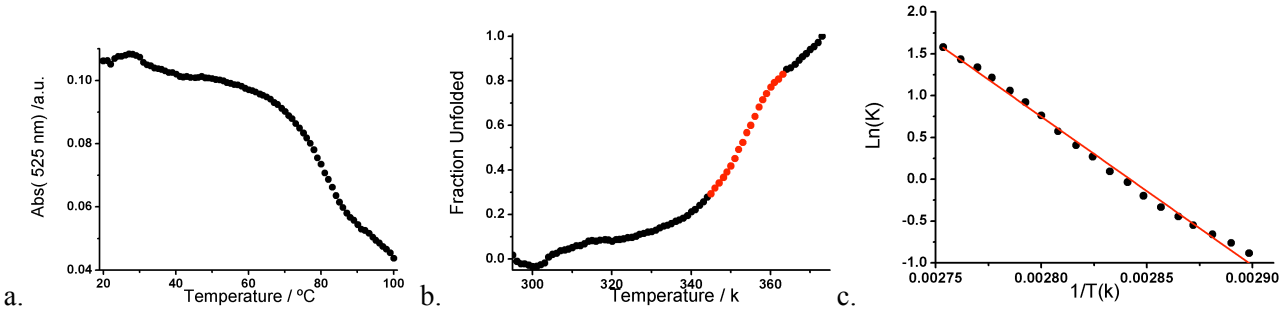

Figure S7. *ΔΔ-[Fe$_2$(**DD-H**)]$^{4+}$: a. Absorbance melting profile at 525 nm; b. Fraction unfolded variation versus temperature; c. Van't Hoff plot.*

11. Fluorescence anisotropy titrations with duplex DNA

A 1 μM solution of the ΛΛ-[Fe_2(**LL-RhH**)]$^{4+}$ helicate in PBS buffer (100 mM / NaCl 100 mM, pH= 7.3) was prepared. Aliquots of a stock DNA solution (34 μM) were sequentially added over the helicate solution, gradually increasing the concentration of DNA in the mixture. The corresponding anisotropy value at 611 nm was recorded after each addition, and the resulting titration profile was analyzed with the *DynaFit* program using a 1:1 binding model including the contribution of higher association complexes.[21]
The experiments were performed at 20 ºC in a 1 cm cuvette (excitation slit: 3 nm; emission slit: 10 nm; integration time 5 s).

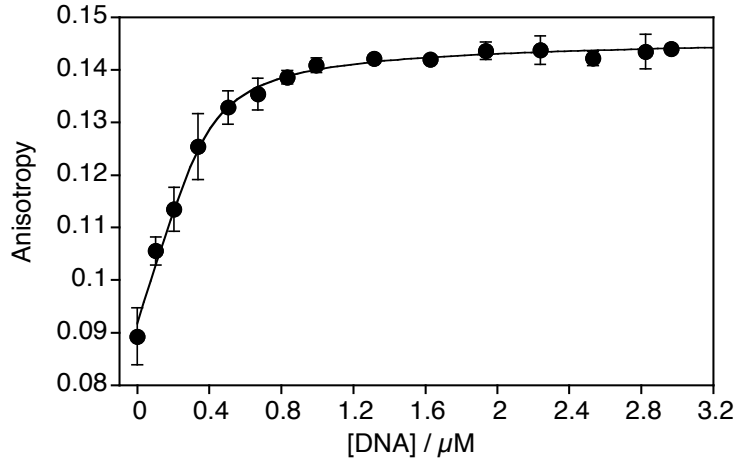

Figure S8. *Anisotropy titration of 1 μM ΛΛ-[Fe_2(**LL-RhH**)]$^{4+}$ helicate in PBS buffer. Experimental points are the mean of three independent experiments, and the curve represents the best fit a 1:1 binding model including the contribution of higher association complexes.*

The resulting dissociation constant for an A/T-rich DNA hairpin is of approximately ≈ 59 μM, which is even weaker than the worse binding constant measured for the mismatched ΔΔ isomer for the three-way junction, thus indicating that the regular B-DNA structure is not a high-affinity target for these type of structures.

12. Binding to Three-way DNA Junctions

Despite the significant chemical differences, the structure of the described peptide helicate is in many ways similar to that of dinuclear supramolecular helicates previously described by Hannon *et. al*;[22] a plausible binding model is based on the reported X-ray structure of the complex between the tetracationic triple helical supramolecular cylinder $[Fe_2(C_{25}H_{20}N_4)_3]Cl_4$ and a three-way DNA junction, as deposited in the PDB database (PDB ID# 2ET0). The minimized structure of the peptide helicate was superimposed with the original metallosupramolecular helicate in the X-ray (specifically, the 2 and 2' carbon atoms in all the coordinating bipyridines were selected for superposition). Inspection of the resulting composite structure does not reveal any major incompatibilities, and in fact shows that the strands of both the organic and the peptide ligands can adopt a similar arrangement inside the three-way junction cavity. Structure superposition was made with the "*Pair Fitting Wizard*" as impolemented in MacPyMOL (PyMOL Molecular Graphics System, v1.6.0.0, Shrödinger LLC).

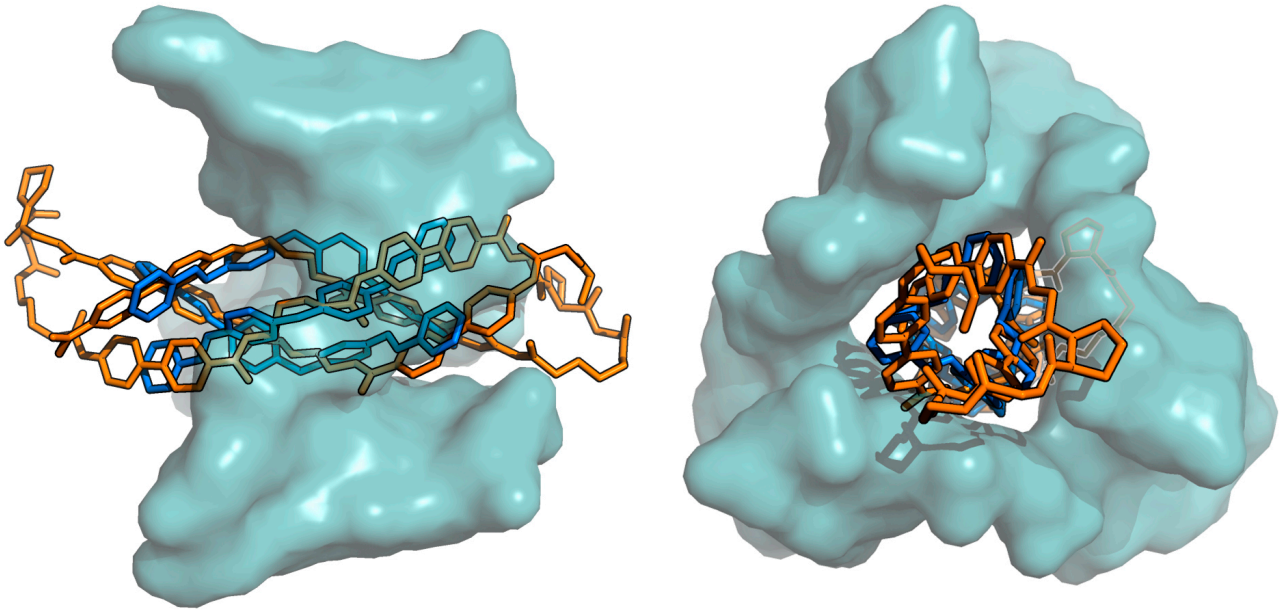

Figure S9. *Result of first-order molecular modeling in which the metallopeptide (orange) is superimposed with the structure of the metallohelicate (blue) in complex with the DNA three-way junction (light blue surface). X-ray data taken from ref. 22.*

13. Cell-internalization studies

Semi-confluent monolayers of Vero cells were grown on glass coverslips in Dulbecco modified Eagle Medium (DMEM) containing 10% of FBS (fetal bovine serum). For the assays, the cells were incubated in DMEM (containing FBS 10%), with compound ΛΛ–$[Fe_2(\mathbf{LL\text{-}RhH})]^{4+}$ (7 μM) overnight at 37 ºC in a 5% CO_2 humidified atmosphere. Then, the cells were gently washed 5 times with PBS and observed under the fluorescence microscope in DMEM without fixation.

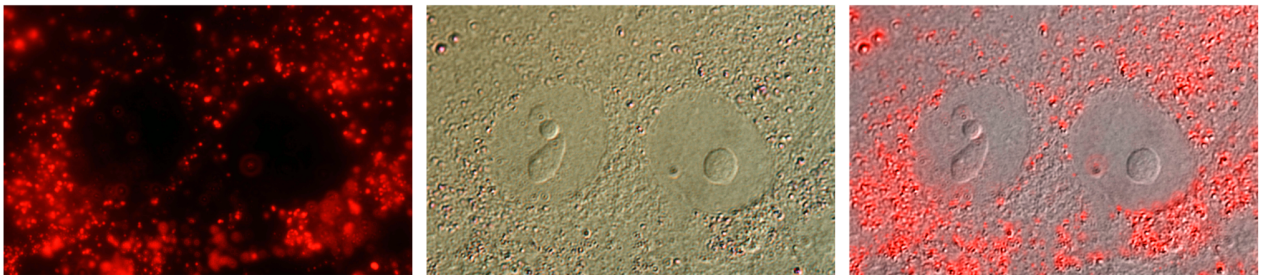

Figure S10. *Vero cells incubated overnight with 7 μM ΛΛ–$[Fe_2(\mathbf{LL\text{-}RhH})]^{4+}$. Left: red channel emission. Middle panel: bright field micrography. Right: Overlay of the two previous images.*

References

1 G. Rama, A. Ardá, J.-D. Maréchal, I. Gamba, H. Ishida, J. Jiménez-Barbero, M. E. Vázquez, M. Vázquez López, *Chem. Eur. J.* 2012, **18**, 7030.

2 G. R. Newkome, J. Gross, A. K. Patri, *J. Org. Chem*. **1997**, *62*, 3013.

3 F. H. Case, *J. Am. Chem. Soc*. 1946, **68**, 2574

4 C. P. Whittle, *J. Heterocyclic Chem*. 1977, **14**, 191.

5 E. F. Pettersen, T. D. Goddard, C. C. Huang, G. S. Couch, D. M. Greenblatt, E. C. Meng, T. E. *J Comput. Chem.* 2004, **13**, 1605.

6 K. Hinsen *J. Comp. Chem.* 2000, **21**, 79.

7 D. A. Case., T. A. Darden., T.E. Cheatham III, C.L. J. Simmerling, R. E. Wang, R. Duke, R. C. Luo, Walker, W. Zhang, K.M. Merz, B. Roberts, S. Hayik, A. Roitberg, G. Seabra, J. Swails, A.W. Goetz, I. Kolossváry, K.F. Wong, F. Paesani, J. Vanicek, R.M. Wolf, J. Liu, X. Wu, S.R. Brozell, T. Steinbrecher, H. Gohlke, Q. Cai, X. Ye, J. Wang, M.-J. Hsieh, G. Cui, D.R. Roe, D.H. Mathews, M.G. Seetin, R. Salomon-Ferrer, C. Sagui, V. Babin, T. Luchko, S. Gusarov, A. Kovalenko, P.A. Kollman (2012), AMBER 12, University of California, San Francisco.

8 J. Wang, R. M. Wolf, J. W. Caldwell, P. A. Kollman, D. A. Case *J. Comput. Chem*. 2004, **25**, 1157.

9 J. Gasteiger M. Marsili *Tetrahedron* 1980, **36**, 3219.

10 L. A. Kelley, S. P. Gardner M. J. Sutcliffe. *Protein Eng*. 1997, **11**, 1063.

11 S. Dapprich, I. Komáromi, K. S. Byun, K. Morokuma, M. J. Frisch *J. Mol. Struct. (Theochem)* 1999, **462**, 1.

12 Gaussian 09, Revision D.01, M. J. Frisch, G. W. Trucks, H. B. Schlegel, G. E. Scuseria, M. A. Robb, J. R. Cheeseman, G. Scalmani, V. Barone, B. Mennucci, G. A. Petersson, H. Nakatsuji, M. Caricato, X. Li, H. P. Hratchian, A. F. Izmaylov, J. Bloino, G. Zheng, J. L. Sonnenberg, M. Hada, M. Ehara, K. Toyota, R. Fukuda, J. Hasegawa, M. Ishida, T. Nakajima, Y. Honda, O. Kitao, H. Nakai, T. Vreven, J. A. Montgomery, Jr., J. E. Peralta, F. Ogliaro, M. Bearpark, J. J. Heyd, E. Brothers, K. N. Kudin, V. N. Staroverov, R. Kobayashi, J. Normand, K. Raghavachari, A. Rendell, J. C. Burant, S. S. Iyengar, J. Tomasi, M. Cossi, N. Rega, J. M. Millam, M. Klene, J. E. Knox, J. B. Cross, V. Bakken, C. Adamo, J. Jaramillo, R. Gomperts, R. E. Stratmann, O. Yazyev, A. J. Austin, R. Cammi, C. Pomelli, J. W. Ochterski, R. L. Martin, K. Morokuma, V. G. Zakrzewski, G. A. Voth, P. Salvador, J. J. Dannenberg, S. Dapprich, A. D. Daniels, Ö. Farkas, J. B. Foresman, J. V. Ortiz, J. Cioslowski, and D. J. Fox, Gaussian, Inc., Wallingford CT, 2009.

13 A. D. Becke *J. Chem. Phys*. 1993, **98**, 5648.

14 C. Lee, W. Yang, R. G. Parr, *Phys. Rev. B* 1988, **37**, 785.

15 A. D. McLean G. S. Chandler, *J. Chem. Phys.* 1980, **72**, 5639.

16 K. Raghavachari, J. S. Binkley, R. Seeger, J. A. Pople *J. Chem. Phys.* 1980, **72**, 650.

17 N. B. Balabanov, K. A. Peterson *J. Chem. Phys.* 2005, **123**, 64107.

18 V. Barone M. Cossi *J. Phys. Chem. A* 1998, **102**, 1995.

19 M. Cossi, N. Rega, G. Scalmani, V. Barone *J. Comp. Chem*. 2003, **24**, 669.

20 T. Vreven, B. Mennucci, C. O. da Silva, K. Morokuma, J. Tomasi *J. Chem. Phys*. 2001, **115**, 62.

21 P. Kuzmic, *Anal. Biochem.*, 1996, **237**, 260.

22 A. Oleksi, A. G. Blanco, R. Boer, I. Usón, J. Aymamí, A. Rodger, M. J. Hannon, M. Coll, *Angew. Chem. Int. Ed.*, 2006, **45**, 1227.